Current density mapping and pinhole imaging in magnetic tunnel junctions via scanning magnetic microscopy

B. D. Schrag[a)]
Micro Magnetics, Inc., 151 Martine Street, Fall River, Massachusetts 02723 and Department of Physics, Brown University, 182 Hope Street, Providence, Rhode Island 02912

Xiaoyong Liu, Weifeng Shen, and Gang Xiao
Department of Physics, Brown University, 182 Hope Street, Providence, Rhode Island 02912

(Received 18 November 2003; accepted 9 February 2004)

We have applied a magnetoresistive microscopy technique to the imaging of current densities and pinhole formation in magnetic tunnel junction devices. In this work, we demonstrate how the magnetic field distribution at the surface of the device can be used to understand the flow of current within the junction itself. By imaging the current-induced fields before and after pinhole formation in several different junctions, we find that many junctions exhibit an unexpectedly complicated current distribution after high-voltage-induced breakdown. Further, we have seen that pinhole locations can be correlated with current inhomogeneities observed before junction breakdown. Finally, we present the results of finite-element simulations which are in good agreement with experimental results. © *2004 American Institute of Physics.* [DOI: 10.1063/1.1695194]

One of the most problematic issues involved in the introduction of devices based on magnetic tunnel junction (MTJ)[1,2] technology is the reduction of the resistance-area product by the fabrication of ever-thinner insulating layers. As the thickness of the tunnel barrier has been decreased below 10 Å, reliability has become a serious issue. The most common failure mechanism for MTJs is the formation of a nanometer-sized conductive short, or ''pinhole,'' between the two ferromagnetic electrodes. Several groups have investigated the properties of insulating barriers and pinholes using a number of different methods, including analysis of current–voltage characteristics,[3–5] imaging of pinholes via decoration[6] or liquid crystal-based methods,[7] and scanning tunneling methods.[8,9] In this work, we present a powerful method of studying current flow and failure in MTJ elements.

For this work, the MTJ samples which were studied had a layer structure, from bottom to top, as follows: Pt 300/Py 30/FeMn 130/Py 60/Al_2O_3 14/Py 120/Pt 200, where Py (permalloy) is $Ni_{21}Fe_{79}$ and thicknesses are given in Å. Here, the tunnel barrier is composed of Al_2O_3 and the Py 60 and Py 120 layers are the pinned and free electrodes, respectively. After deposition, the bottom Pt/Py/FeMn layers are patterned to form a current lead underneath the structure, while the Py/Al_2O_3/Py/Pt layers are patterned and become the MTJ itself. Finally, a 2000-Å-thick layer of gold is deposited over the MTJ and patterned into a top current lead. The patterned layer structure and full MTJ geometry are shown schematically in Figs. 1(a) and 1(b), respectively. In this experiment, the MTJs were patterned into one of a number of shapes, with lateral dimensions ranging from 4 to 50 μm. The resistance-area product for the MTJs was on the order of 4000 $\Omega\cdot\mu m^2$, and each junction had a lead resistance of roughly 140 Ω, which was in general larger than the actual junction resistance R_J (~10–100 Ω, depending on the area).

The physics of the technique, which was described[10] in more detail in an earlier work, is straightforward: a magnetic sensor capable of submicron resolution is raster scanned at the surface of the MTJ, in order to image the current-induced stray magnetic fields at the surface of the sample. These fields are then analyzed to map out lateral current flow within the sample. The technique is nondestructive and can be applied in a magnetic field, opening up several interesting experimental possibilities.

In Ref. 10, we were able to assume that the current flowed in a relatively thin plane, which allowed the use of a simplified algorithm[11] to determine the absolute value of current density in the sample. For magnetic tunnel junction samples, the total thickness of current carrying layers (~3000 Å) is comparable to the sensor-to-sample distance (3000–5000 Å). However, all magnetic field images of interest in this work are created by currents in the much thinner (~400 Å) patterned MTJ tri-layer itself. Therefore, this al-

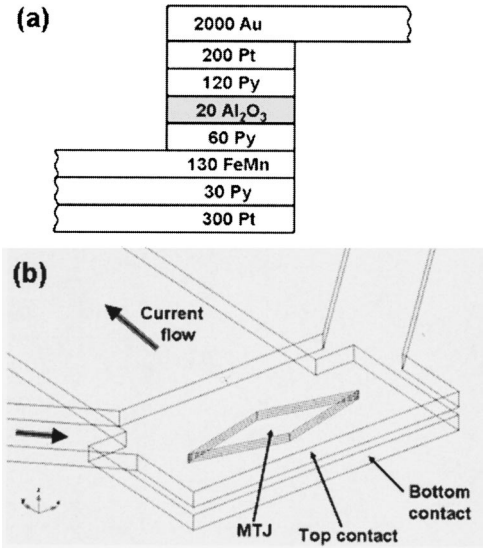

FIG. 1. (a) Schematic of the MTJ layer structure and (b) sketch of the geometry of the devices under test.

[a)]Electronic mail: schrag@micromagnetics.com

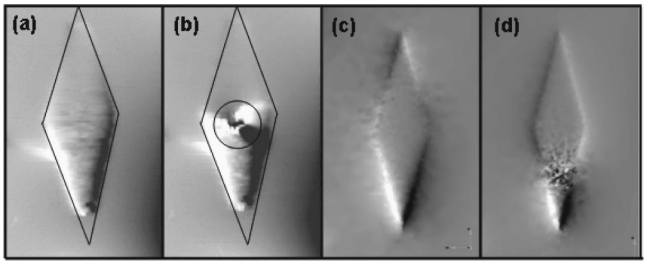

FIG. 2. Measured magnetic field images of a diamond-shaped MTJ device (a) before and (b) after the creation of a pinhole. (c) and (d) Corresponding results from finite-element simulations.

gorithm can still be used to obtain rough estimates of current density.

We present in Figs. 2(a) and 2(b) magnetic field images at the surface of a diamond-shaped MTJ before and after the creation of a pinhole (black lines indicate the outline of the junction area itself). In these and subsequent field images, white (black) areas indicate regions of large positive (negative) magnetic fields. The pinhole in this structure was created by the application of a large ($\sim$2 V) dc voltage across the junction for several seconds. The location of the pinhole in this structure is near the center of the MTJ and is circled. Figures 2(c) and 2(d) show results of finite-element simulations of an identically shaped junction with and without a pinhole of diameter 100 nm. These simulations were performed with the FEMLAB package with $\sim 10^5$ elements.

The experimental and simulated images have many similarities. Figures 2(a) and 2(c) show that undamaged junctions are outlined on either side by white and black. These ''edge fields'' indicate regions of high and low magnetic field, respectively. A junction which has a uniform current flow throughout its cross-sectional area will have no strong fields except at its edges, so a field image which shows only these edge fields and not much else indicates that the junction being imaged is undamaged and behaving as expected. In addition, the strength of these edge field signatures in (a) and (c) is largest at the bottom of the junction and diminishes toward the top of the junction. This effect is due to the fact that current is introduced from a lead at the bottom left of the image. Current injected into the device flows up through the junction, tunnels through the barrier somewhere inside the diamond-shaped MTJ area, and then quickly disperses into the bottom contact, exiting at the left edge of the image. Therefore, almost all the current flow must pass through the bottom-most areas of the junction, but the top regions of the junction will experience a small amount of current flow due only to electrons which happen to tunnel through the very topmost areas of the insulating barrier. As a result, we can expect a MTJ with a perfectly uniform barrier to have a field amplitude at its edges which decreases monotonically from the bottom to the top of the junction.

Turning to Figs. 2(b) and 2(d), we can immediately see that the introduction of a pinhole creates a complicated pattern of strong magnetic fields in its vicinity. It was determined that the pattern of magnetic field poles near the pinhole in the simulated image was caused by the finite mesh size, which effectively discretized the current flow. It is also seen from this and later figures that pinholes can create very complicated field signatures in real devices, where one would expect the current flow not to be limited to discrete paths, at least at the length scales involved (0.1–1 μm). The reason for a more complicated field pattern near a real pinhole is not clear, but it is apparent that the idea of dielectric breakdown as the formation of a tiny, isolated conducting path across the barrier cannot, by itself, explain the behavior observed here.

It can be seen in the simulated image (d) that the edge field amplitude has opposite polarities above and below the pinhole; this implies that current is entering the pinhole from all directions. In both the experimental and simulated images, the amplitude of the edge fields is more or less constant in the regions above and below the pinhole. If some current were flowing through the barrier rather than a pinhole, these amplitudes would change in a smooth fashion in these areas. The fact that the edge field experiences a large change in amplitude only at the pinhole confirms that virtually all of the current is passing through the pinhole, rather than a case in which some current ''bleeds off'' through the insulating barrier. At the pinhole in (b), the high and low field peaks rapidly converge; this is a telltale sign that the electrical current is necking down before passing through the pinhole.

For the results presented in the final two figures, the following procedure was followed. Each MTJ was bonded and imaged, and a hysteresis loop collected. Each MTJ was then stressed in an attempt to induce dielectric breakdown. The voltage across the sample was then ramped at a rate of $\sim$5 mV/s and its resistance monitored until a jump in resistance was observed. The stressing was then ended and a new image and hysteresis loop was collected. This stress-and-image process was repeated until the junction exhibited negligible magnetoresistance.

Figure 3 shows the results of imaging conducted on a 9×36 μm rectangular junction. Images (a) and (c) show the current density image and hysteresis loop taken before dielectric breakdown, while images (b) and (d) show the corresponding data after breakdown, which occurred at a voltage of 0.96 V across the junction. As mentioned earlier, the current density images are imperfect due to limitations inherent in the algorithm used. The most notable inconsistency in these current density images is a ''glow'' just outside the borders of the MTJ itself, which is an artifact of the sample geometry.

Before dielectric breakdown, the current flow is relatively predictable, tending to flow along the left side of the sample (perhaps because both leads into the sample are at the left edge, making the left edge a path of lower resistance), and diminishing as the current flows up the sample. After breakdown, however, image (b) shows a more complicated picture. Some current continues to flow up the left side of the sample, as in (a), but a larger portion of the current is seen to diverge from this path, taking a twisting route through the sample and then vanishing suddenly, at what is undoubtedly the location of a pinhole. This complicated path cannot be explained by the existence of the pinhole by itself, because this twisting path is several microns long and the current flow which is imaged here is in fact taking place in the upper magnetic electrode. If the upper magnetic electrode exhibited damage only in the form of a single nanometer-size pinhole, it seems reasonable that the current flow at any appreciable

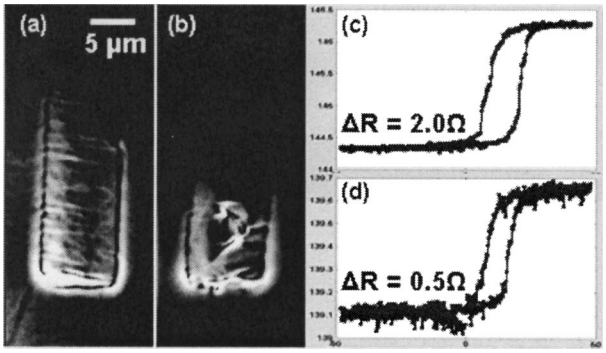

FIG. 3. Current density maps of a $9\times36\ \mu m^2$ rectangular MTJ device (a) before and (b) after dielectric breakdown. (c) and (d) Hysteresis loops taken before and after the device failed.

distance (>500 nm) away from the pinhole would be more uniform and symmetric than what is observed. We plan to investigate this issue in the near future.

The magnetoresistance of this sample was measured to be a quarter of that which was found for the undamaged sample. It can be estimated from (b) that roughly this same fraction of current is still following the original path through the junction area. These two facts taken together lend credibility to the model[12] of a MTJ as a resistor network in which the pinhole can be thought of as a resistor which has been added in parallel with the junction resistance, and that the magnetoresistance of the sample can be calculated from the relative amounts of current flowing through each path. However, Fig. 3 shows that it is not true that the pinhole area must grow to cover the entire junction area as the magnetoresistance drops to zero, as has been suggested.[12] Magnetic field images like those in Figs. 2 and 3 demonstrate that even a pinhole with a small area can have an effective resistance of nearly zero, eliminating all traces of magnetoresistance.

Figure 4 shows current density maps over a $6\times24\ \mu m$ rectangular junction (a) before stressing, (b) after a first period of stressing, and (c) after a second period of stressing. Figures 4(d) and 4(e) show the resistance hysteresis loops of the sample corresponding to images (a) and (c), respectively. This junction showed an initial breakdown at 0.91 V during the first stress period, and exhibited no resistance jump during the second stressing period, due to the fact that an extremely small post-breakdown value of R_J ($\approx1.2\ \Omega \approx0.01R_L$) limited the amount of voltage which could be applied to the junction itself: a maximum voltage of up to 0.2 V, corresponding to roughly 160 mA of current, was applied to the junction during this period. It is noted that, even though this sample showed an 18% magnetoresistance, the initial current density map deviates significantly from the ideal case. The current entering at the bottom of the junction makes three switch-backs before flowing into the remainder of the junction. After the first period of voltage stressing [see Fig. 4(b)], a pinhole is observed in a location of the sample which had exhibited an area of current crowding prior to breakdown. Almost all of the current through the sample flows through this pinhole, in agreement with the huge drop in magnetoresistance. In some other samples, a similar behavior was found, whereby a pinhole formed at a site of previously inhomogeneous current flow. The seeming correlation between pinhole formation sites and the locations of pre-breakdown current bottlenecks will be explored further in a later work.

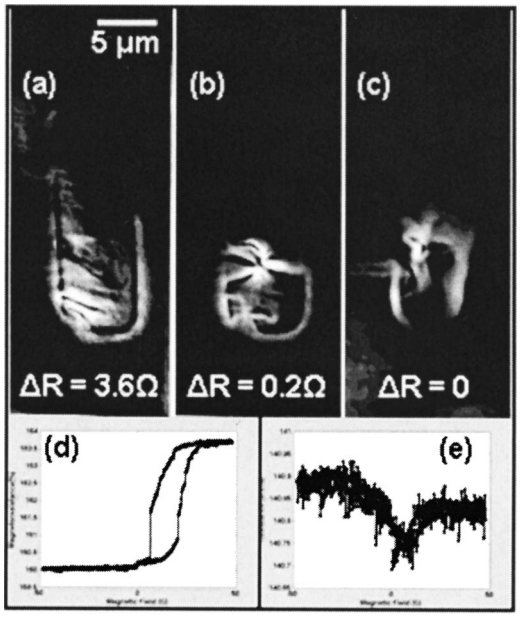

FIG. 4. Current density maps of a $6\times24\ \mu m^2$ rectangular MTJ device (a) before stressing, (b) after an initial period of stressing, and (c) after a second period of stressing. (d) and (e) Resistance hysteresis loops corresponding to images (a) and (c), respectively.

After the second period of voltage stressing, the magnetoresistance drops from roughly 1% to nil, and the subsequent current density image (c) shows dramatic changes in the electron flow through the sample: most of the current still appears to be flowing through the pinhole which is seen in Fig. 4(b), but the path which is taken by this current is much different. One hypothesis for this change is that the intense current, and corresponding heating, applied to the sample has caused extensive damage to the conductive layers above the insulating barrier, forcing the current to flow in a more circuitous fashion around the damaged area.

This work was supported by NSF DMR-0306711 and NSF DMR-0080031.

[1] J. S. Moodera, L. R. Kinder, T. M. Wong, and R. Meservey, Phys. Rev. Lett. **74**, 3273 (1995).
[2] T. Miyazaki and N. Tezuka, J. Magn. Magn. Mater. **139**, L231 (1995).
[3] W. Oepts, H. J. Verhagen, R. Coehoorn, and W. J. M. de Jonge, J. Appl. Phys. **86**, 3863 (1999).
[4] K. Shimazawa, N. Kasahara, J. J. Sun, S. Araki, H. Morita, and M. Matsuzaki, J. Appl. Phys. **87**, 5194 (2000).
[5] J. Das, R. Degraeve, P. Roussel, G. Groeseneken, G. Borghs, and J. D. Boeck, J. Appl. Phys. **91**, 7712 (2002).
[6] D. Allen, R. Schad, G. Zangari, I. Zana, D. Yang, M. C. Tondra, and D. Wang, J. Vac. Sci. Technol. A **18**, 1830 (2000).
[7] W. Oepts, H. J. Verhagen, W. J. M. de Jonge, and R. Coehoorn, Appl. Phys. Lett. **73**, 2363 (1998).
[8] T. Dimopoulos, V. Da Costa, C. Tiusan, K. Ounadjela, and H. A. M. van den Berg, J. Appl. Phys. **89**, 7371 (2001).
[9] E. Z. Luo, S. K. Wong, A. B. Pakhomov, J. B. Xu, I. H. Wilson, and C. Y. Wong, J. Appl. Phys. **90**, 5202 (2001).
[10] B. D. Schrag and G. Xiao, Appl. Phys. Lett. **82**, 3272 (2003).
[11] B. J. Roth, N. G. Sepulveda, and J. P. Wikswo, J. Appl. Phys. **65**, 361 (1989).
[12] B. Oliver, Q. He, X. F. Tang, and J. Nowak, J. Appl. Phys. **91**, 4348 (2002).